applied sciences

MDPI

Article

A Flexible, Low-Cost and Algorithm-Independent Calibrator for Automated Blood Pressure Measuring Devices

José Miguel Costa Dias Pereira [1,2,*], Gonçalo Ribeiro [2] and Octavian Postolache [3]

[1] Escola Superior de Tecnologia, Instituto Politécnico de Setúbal, 2910-761 Setúbal, Portugal
[2] Instituto de Telecomunicações, ISCTE—Instituto Universitário de Lisboa, 1649-026 Lisboa, Portugal; goncalo_tome_ribeiro@iscte-iul.pt
[3] Department of Information Science and Technology, ISCTE—Instituto Universitário de Lisboa, Av. das Forças Armadas, 1649-026 Lisbon, Portugal; octavian.adrian.postolache@iscte-iul.pt
* Correspondence: dias.pereira@estsetubal.ips.pt

Abstract: Arterial hypertension is one of the most important public health problems, especially in developed countries. The quality and calibration of blood pressure (BP) equipment used for non-invasive blood pressure (NIBP) measurement are essential to obtain accurate data that support correct medical diagnostics. This paper includes the hardware and software description of a flexible, low-cost and algorithm-independent calibrator prototype that can be used for the static and dynamic calibration of automated blood pressure measuring devices (ABPMDs). In the context of this paper, the meaning of calibrator flexibility is mainly related to its ability to adapt or change easily in response to different situations in terms of the calibration of ABPMDs that can use a variety of calibration settings without the need to use specific oscillometric curves from different ABPMD manufacturers. The hardware part of the calibrator includes mainly an electro-pneumatic regulator, used to generate dynamic pressure signals with arbitrary waveforms, amplitudes and frequencies, a pressure sensor, remotely connected through a pneumatic tube to the blood pressure (BP) cuff, a blood pressure release valve and analog conditioning circuits, plus the A/D converter. The software part of the calibrator, mainly developed in LabVIEW 20, enables the simulation of oscillometric pressure pulses with different envelope profiles and the implementation of the main algorithms that are typically used to evaluate systolic, diastolic and mean arterial pressure values. Simulation and experimental results that were obtained validate the theoretical expectations and show a very acceptable level of accuracy and performance of the presented NIBP calibrator prototype. The prototype calibration results were also validated using a certified NIBP calibrator that is frequently used in clinical environments.

Keywords: automated blood pressure measuring devices (BPMDs); oscillometric method; electro-pneumatic pressure regulator; calibration; health primary care

check for updates

Academic Editors:
Marius Baranauskas and Piotr Gas

Received: 2 January 2025
Revised: 26 February 2025
Accepted: 12 March 2025
Published: 14 March 2025

Citation: Pereira, J.M.C.D.; Ribeiro, G.; Postolache, O. A Flexible, Low-Cost and Algorithm-Independent Calibrator for Automated Blood Pressure Measuring Devices. *Appl. Sci.* **2025**, *15*, 3198. https://doi.org/10.3390/app15063198

Copyright: © 2025 by the authors. Licensee MDPI, Basel, Switzerland. This article is an open access article distributed under the terms and conditions of the Creative Commons Attribution (CC BY) license (https://creativecommons.org/licenses/by/4.0/).

1. Introduction

A recent report from the World Health Organization, dated March 2023, states that hypertension affects 1.28 billion adults aged 30–79 years worldwide, that an estimated 46% of adults with hypertension are unaware that they have the condition, that less than half of adults (42%) with hypertension are diagnosed and treated and that hypertension is a major cause of premature death worldwide [1–6]. Thus, blood pressure measurement (BPM) has a real impact on the welfare of the worldwide population, on people's quality of life and on the reduction in the large costs associated with the control and treatment of this disease.

Regarding BPM accuracy, it is important to note that the current gold standard is through intra-arterial measurement, but this is an impractical method in ambulatory conditions due to its highly invasive nature. Therefore, practically all clinical institutions rely on indirect alternatives, and office BP measurements are mostly performed using automatic oscillometric devices with a brachial cuff. However, most of the automated blood pressure measuring devices (ABPMDs) do not prove accurate readings according to international validation standards [7], and their regular test and calibration are essential. Moreover, currently, there are many thousands of unique automated BPMDs from different manufacturers, each one using proprietary and empirical algorithms to estimate BP parameters [8–10]. Thus, each manufacturer creates its own pressure curves or envelopes for NIBP measurement, which are sometimes referred to as O′ curves, that are specific to a particular NIBP monitor. Those curves, obtained during the deflation phase of the cuff, are a graphical representation of the sensed pressure oscillation amplitude variations during the linear decreasing cuff air pressure [11,12]. This paper proposes a low-cost NIBP calibrator that creates specific envelope profiles that provide an algorithm-independent calibration of ABPMDs using a common envelope profile for which the different ABPMDs give the same measurement results if they use the same BP evaluation algorithm type, being it the fixed ratio or the maximum slope algorithm. In this way, the proposed NIBP calibrator prototype, which will be presented in this paper, enables the evaluation of the fixed heigh ratios implemented by different ABPMD manufacturers and also enables us to check the differences between different devices in terms of implemented algorithms. Regarding comparisons with similar studies, it will be worth highlighting the EU-funded research project adOSSIG [13] that aims to improve the reliability and accuracy of blood pressure (BP) measurements by developing an interesting oscillometric signal generator (OSG). In this project, the hardware solution that is presented for an oscillometric signal generator is capable of generating oscillometric blood pressure pulses that pretend to be indistinguishable from real physiological human signals [14]. However, the research that is developed by adOSSIG is more centered in hardware issues than in software issues. The proposed simulator is developed considering a large database of physiological signals recorded from healthy patients and people with heart diseases and aims to achieve a reliable reproduction of those signals. Thus, the referred research project does not present any new methodologies to test ABPMDs but proposes specific oscillometric pulse envelopes to obtain an independent algorithm calibrator of the empirical algorithm used by each ABPMD. There are also a significative number of papers [15–17] that present other solutions for the implementation of an ABPMD calibrator, but almost in all of them, the performance evaluation of the proposed solutions requires clinical validation and the usage of a significant group of persons and trained medical staff. These requirements are expensive, not immune to different error types and time consuming in terms of data acquisition. Regarding the flexibility of the proposed calibrator, the following capabilities can be underlined: it is possible to specify the calibration mode, manual or automatic; to configure the calibration to be performed with any of the most common oscillometric algorithms (systolic/diastolic rates or maximum/minimum slope); to define the different parameters of the pulse envelope pressure signal; to generate artificial pulse waveforms and pulse envelopes that mimic physiological BP signals with specific characteristics, such as the typical oscillometric pulse envelope BP of people that suffer from heart arrhythmia, arteriosclerosis, very high or low BP values, or other heart diseases; and to perform ABPMD sensitivity tests using variable maximum envelope amplitudes that can vary between 1 and 50 mmHg, with a 0.1 mmHg resolution. The paper is organized as follows: part one, already presented, is the introduction; part two presents the common oscillometric blood pressure estimation algorithms and also the proposed method to implement an algorithm-independent calibrator of ABPMDs; part three presents

the hardware and software descriptions of the developed prototype; part four includes the simulation and experimental results; and the last part, part five, is dedicated to conclusions.

2. Oscillometric Blood Pressure Estimation Algorithms

The oscillometric BP measurement technique is based on the measurement values obtained from a pressure transducer that is connected to the arm cuff. The pressure oscillation peaks around the mean arterial pressure (MAP) are processed by proprietary algorithms, yielding the systolic and diastolic pressures. The most popular empirical algorithms used to evaluate BP values from ABPMDs are the maximum amplitude, derivative, and fixed ratio algorithms [18,19]. The maximum amplitude algorithm estimates mean BP as the external pressure at which the BP oscillogram has a peak value [20,21]. Then, using interpolating algorithms, such as polynomial or spline interpolation algorithms, the fixed ratio algorithm estimates each diastolic BP and systolic BP reading as the external pressure at which the BP oscillogram is at some fraction of its peak value [22]. Another algorithm that is also commonly used is the derivative algorithm, which estimates diastolic BP and systolic BP as the external pressures at which the oscillogram interpolated peak curve has its maximum and minimum slopes, respectively [23,24]. It is important to underline that these algorithms are proprietary [25,26] and are not commonly divulgated by ABPMD manufacturers. Figure 1 includes a graphical representation of the key values that are used to evaluate the systolic and diastolic BP values based on the BP oscillogram peak envelope.

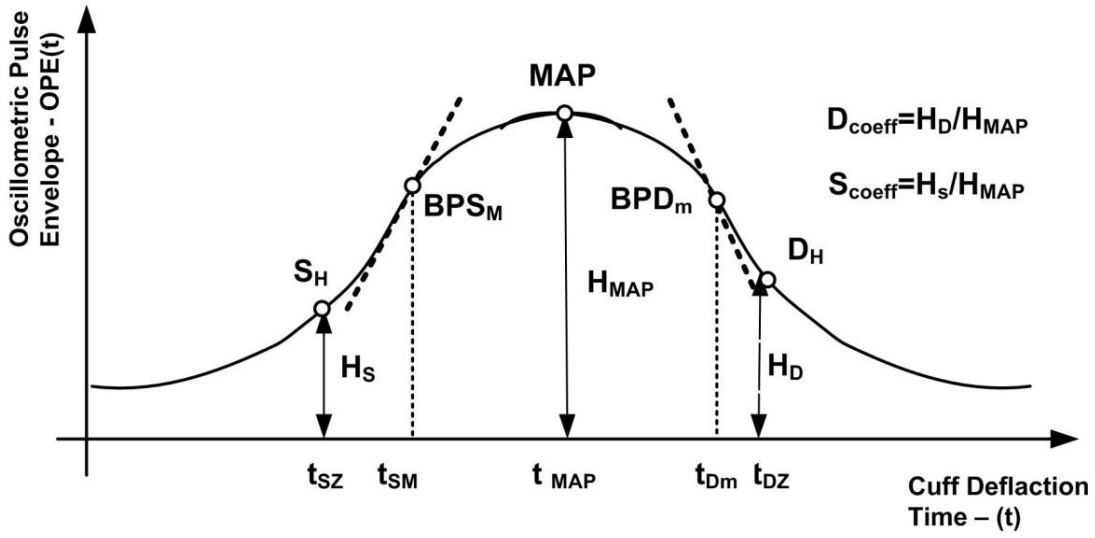

Figure 1. Graphical representation of the key values involved in the fixed ratio and maximum slope algorithms (MAP—mean arterial pressure; S_H—systolic pressure obtained by using the fixed ratio algorithm; D_H—diastolic pressure obtained by using the fixed ratio algorithm; S_M—systolic pressure obtained by using the maximum slope algorithm; D_H—diastolic pressure obtained by using the maximum slope algorithm; H_{MAP}—oscillometric pulse envelope amplitude associated with mean arterial blood pressure; H_S—oscillometric pulse envelope amplitude associated with systolic blood pressure; H_D—oscillometric pulse envelope amplitude associated with diastolic blood pressure; S_{coef}—systolic coefficient used in the fixed ratio algorithm; D_{coef}—diastolic coefficient used in the fixed ratio algorithm).

Thus, to implement an algorithm-independent calibrator of ABPMDs, three specific pulse envelope profiles are considered, namely, the triangular, the trapezoidal and the parabolic pulse envelope profiles. Basically, the objective of each one of the envelope profiles is to create a reference profile that generates a similar measurement of the BP parameters independently of the specific algorithm used in the ABPMD under test. Taking as an example the sphygmo-

manometer pressure curve represented in Figure 2, the variables that are used to synthesize the different envelope profiles are as follows: PM, maximum cuff pressure (mmHg); Pm, minimum cuff pressure (mmHg) during the deflation phase; dT, duration of the deflation phase (s); SBP, systolic blood pressure (mmHg); DBP, diastolic blood pressure (mmHg); MAP, mean arterial blood pressure (mmHg); HBR, heart beat rate (b.p.m.); amp, amplitude of the pressure pulses (mmHg); and SR, sampling rate (S/s). In the same figure, dT represents the duration of the deflation phase, d_up represents the duration of the inflation phase and d_down represents the duration of the release phase, which are the three pressure variation phases associated with the cuff pressure curve.

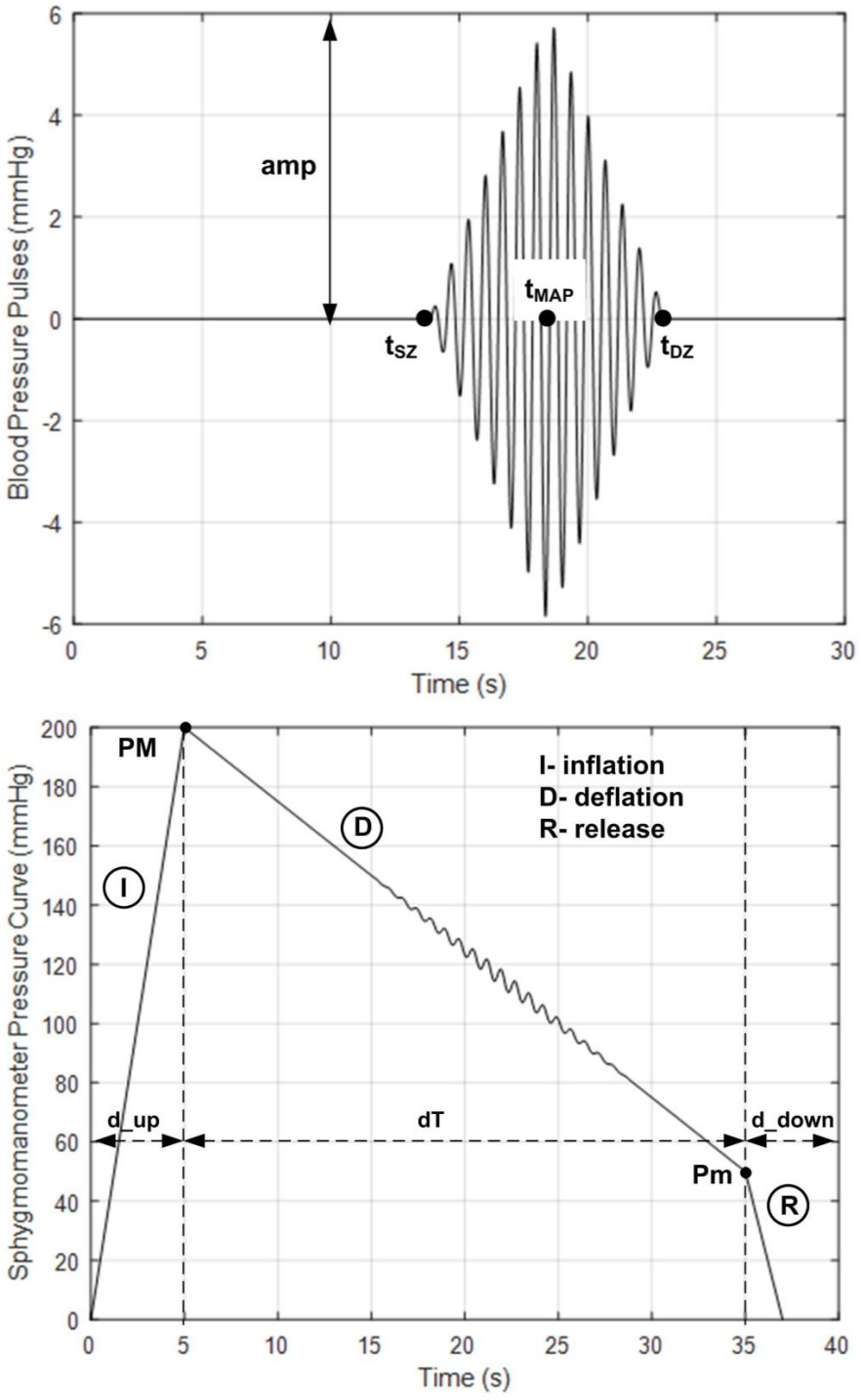

Figure 2. Synthesized cuff pressure curve (PM = 200 mmHg; Pm = 50 mmHg;; MAP = 100 mmHg; dT = 30 s; d_up = 5 s; d_down = 5 s; amp = 6 mmHg).

As an example, Figure 3 represents a triangular pulse envelope associated with the following set of simulation parameters: dT = 30 s; SBP = 120 mmHg; DBP = 80 mmHg; MAP = 100 mmHg; HBR = 90 b.p.m. and amp = 6 mmHg. When this envelope profile is used to calibrate an ABPMD, since there is a linear and continuous variation in the pulse amplitudes between 0 and its maximum value, it is possible to obtain, based on the measurements of the ABPMD, the values of the height coefficients used in the fixed ratio algorithm, but obviously only if this is the algorithm implemented to evaluate the BP parameters. The values of the simulation parameters used to synthesize the triangular pulse envelope are obtained from the following set of relationships:

$$t_{SZ} = \frac{PM - SBP}{m}$$

$$t_{DZ} = \frac{PM - DBP}{m}$$

$$t_{MAP} = \frac{PM - MBP}{m}$$

where m represents the slope of the linear interpolation of the deflation pressure variation, given by

$$p(t) = PM - m{\cdot}t \; where \; m = \frac{PM - Pm}{dT}$$

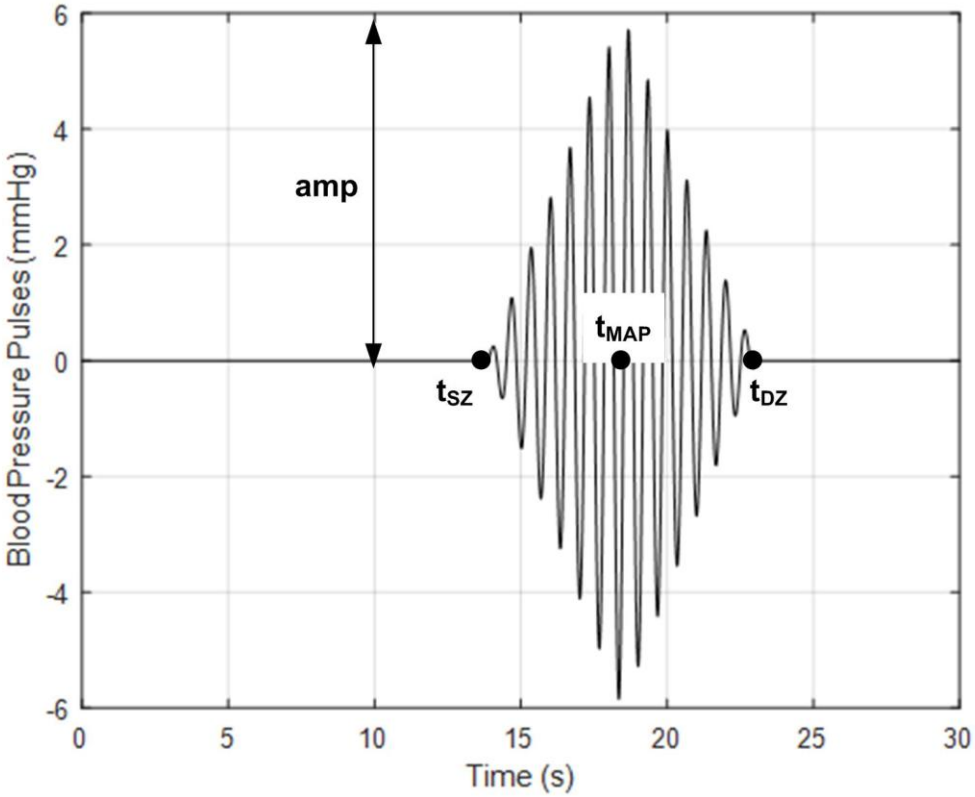

Figure 3. Triangular pulse envelope to be used in the evaluation of the systolic and diastolic height coefficients when using the fixed ratio algorithm.

According to the readings obtained from the ABPMD under evaluation, the coefficients that are used to implement the fixed ratio algorithm are given by

$$D_{coeff} = \frac{H_D}{H_{MAP}}$$

$$S_{coeff} = \frac{H_S}{H_{MAP}}$$

where H_D/H_{MAP} and H_S/H_{MAP} represent the ratio values used to evaluate the diastolic and systolic pressures, respectively. These coefficient values can then be checked out and compared with the typical values used by the fixed ratio algorithm [24,27,28].

As an example, Figure 4 represents a trapezoidal pulse envelope associated with the following set of simulation parameters: dT = 30 s; SBP = 120 mmHg; DBP = 80 mmHg; MAP = 100 mmHg; HBR = 90 b.p.m. and amp = 6 mmHg. When this envelope profile is used, it is possible check the correct operation of any ABPMD that uses the fixed ratio algorithm if S_{coeff} and D_{coeff} are higher than the coefficients used in the fixed ratio algorithm, which are typically lower than 0.7 [29,30]. If this is the case, the measured values are ideally equal to SBP and DBP, respectively.

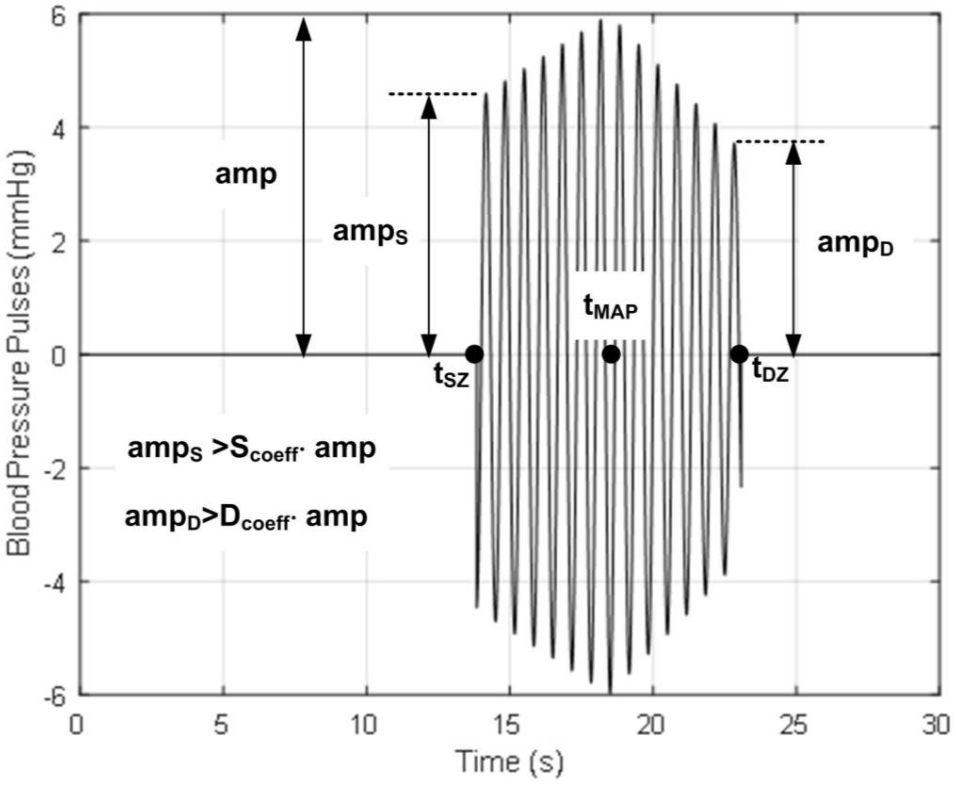

Figure 4. Trapezoidal pulse envelope to be used in the evaluation of the systolic and diastolic pressures when using the fixed ratio algorithm.

Finally, also as an example, Figure 5 represents a parabolic pulse envelope associated with the following set of simulation parameters: dT = 30 s; SBP = 120 mmHg; DBP = 80 mmHg; MAP = 100 mmHg; HBR = 90 b.p.m. and amp = 6 mmHg. When this envelope profile is used, it is possible to check the correct operation of any ABPMD that uses the maximum slope algorithm since the maximum and minimum slopes occur for t_{SM} and t_{Dm}, respectively. If in this case the measured values are ideally equal to SBP_M and DBP_m, respectively, the coefficients BPS_M, BPD_m, t_{SM} and t_{Dm} are defined by

$$\left(\frac{d(OPE(t)}{dt}\right)_{Max} \text{ is maximum for } BP = BPS_M \text{ and } t = t_{SM}$$

$$\left(\frac{d(OPE(t)}{dt}\right)_{Min} \text{ is minimum for } BP = BPD_m \text{ and } t = t_{Dm}$$

where the OPE(t) represents the oscillometric pulse envelope represented in Figure 1.

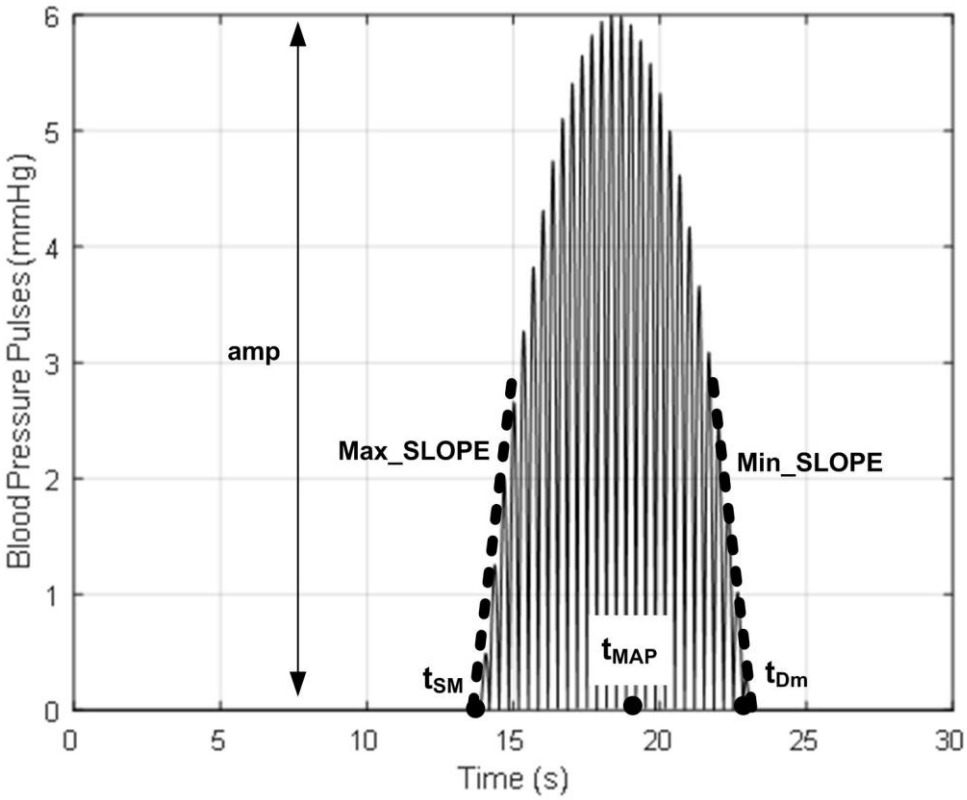

Figure 5. Parabolic pulse envelope to be used in the evaluation of the systolic and diastolic pressures when using the maximum slope algorithm.

3. System Description

3.1. Hardware

Figure 6 represents the hardware block diagram of the proposed measurement system. The hardware includes a piezoresistive gauge pressure transducer [31] that is used in a wide range of applications, namely biomedical applications, such as NIBP measurement. One specific feature of the pressure transducer is its temperature compensation capability in the temperature range between −40 °C and +125 °C, this being the compensation important to minimize errors caused by temperature variations. The signal conditioning circuit (SC) of the oscillometric pulse signal has an automated gain control (AGC) feature implemented by a digital potentiometer, and this feature can be used to adjust the measurement's sensitivity. The two main electro-pneumatic components in the hardware part of the prototype include an electro-pneumatic pressure regulator (EPPR), which is used to generate pressure signals for static and dynamic calibration purposes [32], and a release valve [33], which is mainly used to depressurize the cuff after the deflation BP measurement phase.

Data processing, control and transmission interface capabilities are provided by a microcontroller [34] that includes an 8-bit microprocessor and a wireless transmission interface that can give access to a Wi-Fi network. To perform the calibration of the pressure sensor and SC circuits, the following components are used: a pressure gauge [35]; a digital multimeter [36]; a data acquisition board [37] and a pressure calibrator [38]. Table 1 summarizes the specifications of the main electrical components and devices that were used.

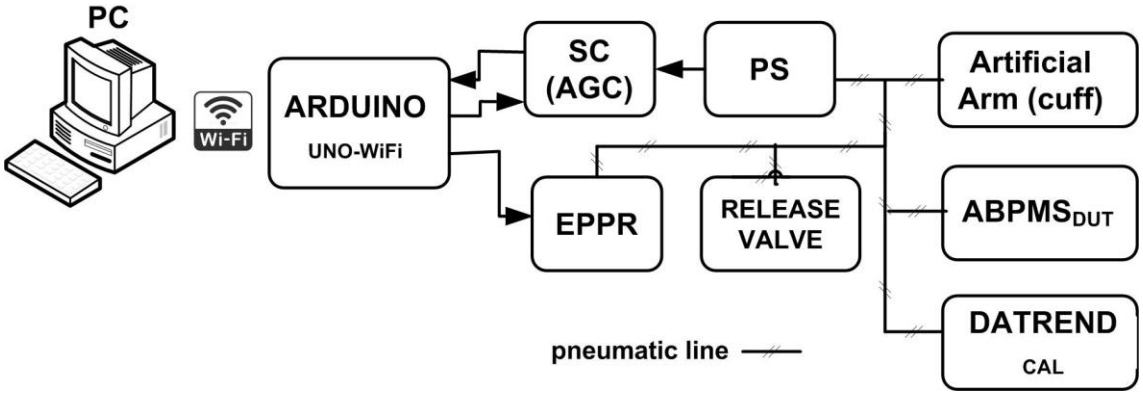

Figure 6. Hardware block diagram of the proposed measurement system (SC—signal conditioning; AGC—automatic gain control; PS—pressure sensor; DUT—device under test; CAL—calibrator; EPPR—electro-pneumatic pressure regulator).

Table 1. Summary of the specifications of the main electrical components and devices.

Component/Device/Reference	Main Specifications
Pressure Sensor NXP SEMICONDUCTORS MP3V5050	measures pressure range between 0 and 50 kPa; 2.5% maximum error relative to V_{FSS}, whose typical value is equal to 2.7 V; sensitivity equal to 54 mV/kPa; response time equal to 1.0 ms and temperature compensation capabilities in the temperature range between −40 °C and +125 °C
Electro-Pneumatic Pressure Regulator (EPPR) PARKER-OEM-P	pressure range between 0 and 5 p.s.i.; control voltage of 0–5 V; monitor output voltage 0–5 V; pressure accuracy of ±1.5% of full-scale maximum; response time lower than 15 ms; linearity better than 1.5% of full-scale maximum and availability of internal vent
Pressure Calibrator DRUCK DPI611	pressure range between −1 and 1 bar; accuracy of 0.0185% of FS and total uncertainty of 0.025% of FS
Release Valve KOGE KSV05	exhaust time lower than 6.0 s for a pressure reduction from 300 mmHg to 15 mmHg; resistance 100 Ω ± 10% and leakage maximum of 3 mmHg/min for a pressure equal to 300 mmHg
Data Acquisition Board National Instruments MYDAQ	two differential analog input channels with 16-bit resolution; maximum sampling rate of 200 kS/s; timing resolution of 10 ns; analog input range ±2 V and ±10 V and typical accuracy of 4.9 mV for analog input range ±2 V
Digital Multimeter Keithley 2000 SERIES	a total of 6 ½ digits; minimum voltage resolution of 0.1 µ for 100 mV scale; linearity for 10 V DC range equal to ±(1 ppm of reading + 2 ppm of range) and accuracy for a DC voltage range from 100 nV to 1 kV equal to 0.002%

Figure 7 represents the block diagram of a multiple pressure sensor calibration platform that was developed to calibrate, simultaneously and in a comparative mode, a set of four different pressure sensors. It is also important to underline that the calibration platform includes a pneumatic line that can have different lengths and diameters, with it being possible to calibrate the entire pressure measuring chain and not only the pressure sensor. This feature can be very important since the accuracy of the ABPMD measurements is affected not only by the pneumatic tube cuff position but also by its length and diameter [39].

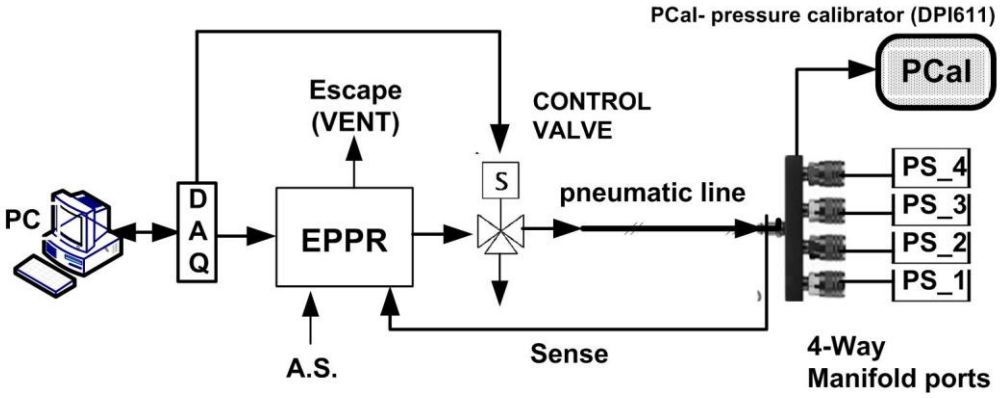

Figure 7. Hardware block diagram of a multiple pressure sensor calibration platform (DAQ—data acquisition board; EPPR—electro-pneumatic pressure regulator; A.S.—air supply; PCal—pressure calibrator; PS—pressure sensor; S—solenoid valve actuator).

3.2. Software

The LabVIEW graphical programming language was used to develop the main routines included in the software part of the proposed prototype. In addition to the generation of the different pulse envelope profiles used for the evaluation of NIBP measurement parameters using the amplitude ratio and the maximum slope algorithms, the proposed NIBP simulator and analyzer also includes routines to perform the following tasks: static pressure tests, leak tests and algorithm-independent BP calibrations. There are also routines to record the measurement data, to generate arbitrary waveform pressure signals with specific pulse envelope parameters and to represent the pressure signals that are used for calibration purposes and the BP oscillometric pulses whose profile is selected according to the algorithm-selected BP parameter evaluation. As an example, Figure 8a,b represent two graphics contained in the panel of the developed software. Figure 8a represents the cuff pressure variation during the three phases of a BP measurement: the pressure inflation phase, which occurs between 0 and 5 s, the pressure deflation phase, which occurs between 5 and 35 s, and the pressure release phase, which occurs between 35 and 37 s. In this example, the maximum cuff pressure is equal 180 mmHg, obviously higher than the SBP used for simulation that is equal 150 mmHg, and the cuff pressure during the release is equal 50 mmHg, obviously lower than the DBP used for simulation that is equal 100 mmHg. Regarding Figure 8b, it represents the BP oscillometric pulse for a trapezoidal pulse envelope associated with a maximum pulse amplitude equal to 3 mmHg and an MAP equal to 120 mmHg.

For the same example that was previously considered, the upper part of Figure 9 displays the graphical representation of the pressure peaks of the oscillometric signal, and the lower part of the figure represents the numerical values that were evaluated for different BP parameters, obtained after processing the previous signal. It can be easily confirmed that the evaluated parameters are very near the theoretical values used for the simulated cuff pressure signal.

The main routines that were developed to generate the calibration signal are the following: synthesis of the complete BP signal, which includes the inflation pressure variation, the deflation pressure variation plus the small amplitude BP pulses, and the pressure variation of the measuring release phase. All timing and amplitude parameters of the synthesized cuff pressure curve, represented in Figure 2, can be adjusted by the user according to the purpose of the calibration to be performed. On the other hand, the main routines that were developed to acquire the BP signal are the following: signal filtering and outlier removal, extraction of the BP pulse envelope, either the fixed ratio algorithm or the derivative algorithm, and routines associated with signal display, data storage, and

data transmission. It is also important to note that, regarding signal processing routines, particular attention must be paid to the usage of filters and other processing operators to minimize measurement errors caused by signal amplitude and phase distortions. Thus, for example, the smoothing of the oscillometric waveform was performed using the Savitzky–Golay filter [40] to ensure that the pulse shape remained preserved in terms of peak amplitudes, positions, widths and areas.

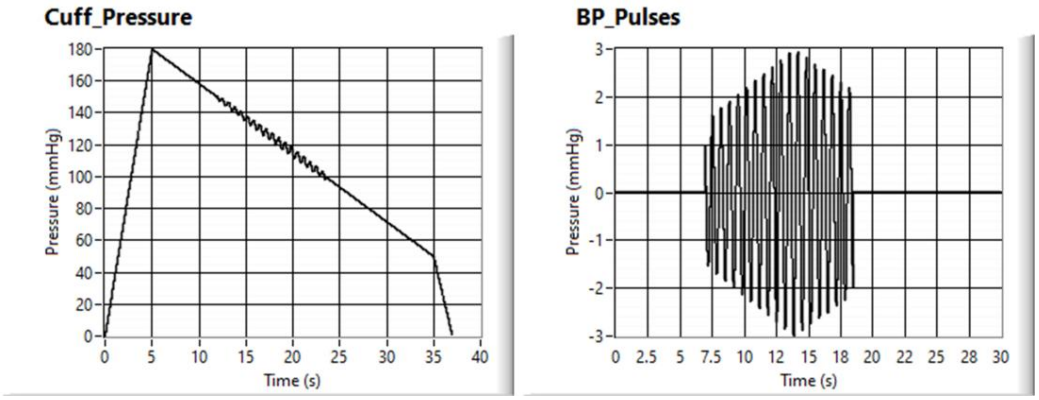

(**a**) (**b**)

Figure 8. Example of two graphics contained in the LabVIEW front panel: (**a**) cuff pressure variation during the three phases of BP measurement; (**b**) BP oscillometric pulse for a trapezoidal pulse envelope associated with a maximum pulse amplitude equal to 3 mmHg and an MAP equal to 120 mmHg.

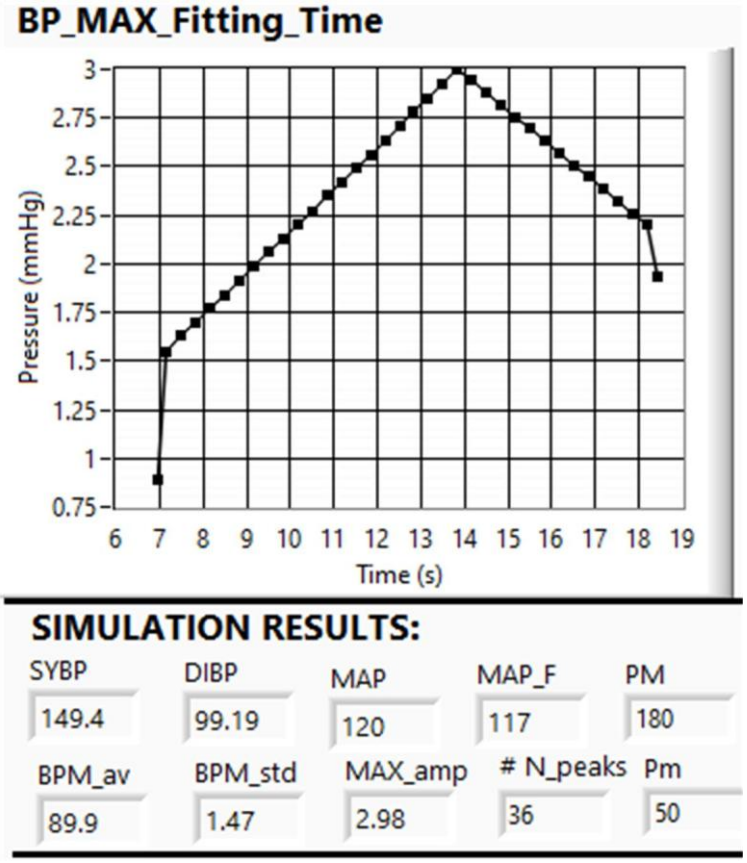

Figure 9. Graphical representation of the pressure peaks of the oscillometric signal and numerical values evaluated for different BP parameters for the simulated cuff pressure signal (PM = 180 mmHg; Pm = 50 mmHg; dT = 30 s; SBP = 150 mmHg; DBP = 100 mmHg; MAP = 120 mmHg; HBR = 90 b.p.m.; amp = 3 mmHg).

4. Experimental Results

This section includes two parts: one part is related to prototype loop tests and the other part is related to prototype performance evaluation. In the first part, the tests that were carried out are based on a feedback configuration of the NIBP calibrator prototype, which means that the output pressure signals generated by the EPPR were acquired and processed by the pressure acquisition part of the prototype. This includes essentially the pressure sensor, the data conditioning circuits and the associated data processing routines that evaluate the measured BP parameters. In the second part, the tests that were carried out include the following: a comparative analysis of the calibration results of a previously calibrated ABPMD [41] using the proposed calibrator prototype, already presented, and a commercial and certified BP calibrator [42] that performs dynamic blood pressure simulations of ABPMDs and also static calibration, automated leak testing, and high- and low-pressure release verifications of those devices.

4.1. Prototype Loop Tests

To evaluate the stand-alone performance of the developed prototype, a loop connection between the output of the pressure signal generator and the input of the pressure signal acquisition of the prototype parts was established. The tests that were performed evaluated the measurement errors caused by the variations in the following parameters: SBP, DBP and MAP; pulse envelope amplitude (AMP_{pulse}); heartbeat rate per minute (HBR_M); mean and standard deviation values; and the data acquisition sampling rate (SR). As an example, Table 2 represents the absolute and relative errors of the evaluation of the SBP, DBP, MAP and HBR_M parameters for a synthesized oscillometric trapezoidal pulse envelope whose SBP, DBP and MAP, together with the maximum amplitude of the oscillometric pulses (AMP) values, were pre-defined as the values that appear in the first column of the table (SBP_DBP_MAP_AMP). The other parameters that were used for simulation purposes had the following values: PM = 180 mmHg, Pm = 50 mmHg, HBR_M = 90 b.p.m, dT = 30 s and SR = 100 S/s. The last column of the table (N_Peaks) represents the number of oscillometric pulses that were detected by the fixed ratio algorithm and then used to evaluate the BP parameters that are represented in columns two, three and four of Table 2. As can be easily verified from the table, the absolute error of the BP parameters that were evaluated is always lower than 1.8 mmHg, a value that is well below the pass clinical validation criterion defined by the British Hypertension Society (BHS), which is equal to 5 mmHg.

Table 2. Absolute and relative errors of the evaluation of the SBP, DBP, MAP and HBR_M parameters for a synthesized trapezoidal pulse envelope whose SBP, DBP, MAP and AMP values appear in the first column of the table.

SBP_DBP_MAPAMP	SBP	DBP	MAP	Absolute Error (mmHg)			Relative Error (%)			HBR_M (av)	HBR_M (std)	N_Peaks
				SBP	DBP	MAP	SBP	DBP	MAP			
120_80_100_3	121.2	81.1	100.2	1.2	1.1	0.2	1.0	1.3	0.2	88.1	1.2	28
120_80_100_6	120.1	81.5	100.4	0.1	1.5	0.4	0.1	1.9	0.4	90.7	0.2	29
125_85_100_3	123.4	84.6	100.4	−1.6	−0.4	0.4	−1.3	−0.5	0.4	91.8	0.4	28
125_85_100_6	124.2	86.8	100.5	−0.8	1.8	0.5	−0.6	2.1	0.5	91.1	0.4	28
135_90_100_3	133.4	90.8	99.7	−1.6	0.8	−0.3	−1.2	0.9	−0.3	91.5	0.3	32
135_90_100_6	135.5	88.8	100.4	0.5	−1.2	0.4	0.4	−1.3	0.4	89.1	0.3	32
150_100_120_3	149.7	101.4	120.3	−0.3	1.4	0.3	−0.2	1.4	0.3	90.0	1.5	35
150_100_120_6	148.8	98.9	120.4	−1.2	−1.1	0.4	−0.8	−1.1	0.3	91.7	8.9	35

Another set of experimental results is presented in Table 3. This table represents the absolute and relative errors of the evaluation of the SBP, DBP, MAP and HBR_M param-

eters for a synthesized oscillometric trapezoidal pulse envelope with SBP = 120 mmHg, DBP = 80 mmHg and MAP = 100 mmHg when the maximum amplitude of the oscillometric pulses (AMPs), which appear in the first column of the table (AMP), varies between 1 mmHg and 6 mmHg, with increments of 1 mmHg. The other parameters used for simulation purposes had the following values: PM = 180 mmHg, Pm = 50 mmHg, HBR_M = 90 b.p.m, dT = 30 s, and SR = 50 S/s (instead of value that was previously used, which was equal to 100 S/s). As previously referred to, the last column of the table (N_Peaks) represents the number of oscillometric pulses that were detected by the fixed ratio algorithm. In this case, for the lowest amplitude value of the oscillometric pulses, namely for AMP = 1 mmHg, which is an extremely low value in real measurement scenarios, the absolute error of the BP parameters reaches 11.6 mmHg, and it is not even possible to evaluate the HBR_M parameter (NaN) for the lower AMP value of 1 mmHg. Thus, for AMP = 1 mmHg and SR = 50 S/s, the absolute is higher than ±5 mmHg. However, if the sampling rate is incremented to 100 S/s, the previous error of 11.6 mmHg is reduced to 2.6 mmHg, with the BHS criterion being verified. At the same time, it becomes possible to evaluate the HBR_M parameter, with the evaluated value being equal to 86.8 b.pm, which is 3.6% below the simulated value of 90 b.p.m.

Table 3. Absolute and relative errors of the evaluation of the SBP, DBP, MAP and HBR_M parameters for a synthesized oscillometric trapezoidal pulse envelope with SBP = 120 mmHg, DBP = 80 mmHg, MAP = 100 mmHg and HBR = 90 b.p.m. when the maximum amplitude of the oscillometric pulses (AMP) varies between 1 mmHg and 6 mmHg.

AMP	SBP	DBP	MAP	Absolute Error (mmHg)			Relative Error (%)			HBR_M (av)	HBR_M (std)	N_Peaks
				SBP	DBP	MAP	SBP	DBP	MAP			
1	108.4	91.6	100.0	−11.6	11.6	0.0	−9.7	14.5	0.0	NaN	0.0	10
2	123.1	83.6	99.8	3.1	3.6	−0.2	2.6	4.4	−0.2	87.9	1.0	28
3	120.3	78.8	99.3	0.3	−1.2	−0.7	0.3	−1.5	−0.7	91.4	0.5	29
4	121.4	81.0	99.3	1.4	1.0	−0.7	1.2	1.2	−0.7	88.1	0.2	29
5	118.2	81.7	100.2	−1.8	1.7	0.2	−1.5	2.1	0.2	90.3	0.3	29
6	120.7	81.7	99.9	0.7	1.7	−0.1	0.6	2.1	−0.1	89.2	0.2	28

4.2. Prototype Performance Evaluation

To evaluate the performance of the developed prototype, a previously calibrated ABPMD [41] was considered and a comparison between the calibration results that were obtained with the proposed prototype and the calibration results obtained with a commercial and certified BP calibrator [41,43] was performed. Regarding the ABPMD that was used to compare the experimental calibration results, it is important to note that this BP monitor is clinically validated in accordance with multiple certified entities, which includes the European Society of Hypertension (ESH) and the German Association for High Blood Pressure (DHL), among others. The commercial and certified BP calibrator that was used for the comparative performance evaluation is a modular calibrator. It is very versatile and supports the maintenance and calibration of NIBP equipment from the simplest commercial ABPMD for home usage to highly accurate equipment used in hospital intensive care units [44]. The previously referred to NIBP monitor has the following main specifications: NIBP measurement capability using the oscillometric algorithm; capability to measure the cardiac rate in the range between 20 and 240 beats per minute (BPM) with an accuracy equal to ±0.25 BPM; minimum diastolic blood pressure measurement capability of 15 mmHg and maximum systolic pressure measurement capability of 275 mmHg. The

BP monitor can also generate regulated pressure signals in the range between 10.0 and 400.0 mmHg with an accuracy of ±0.5 mmHg and has a resolution of 0.1 mmHg. Figure 10 depicts the test setup that was used to calibrate the home blood pressure monitor.

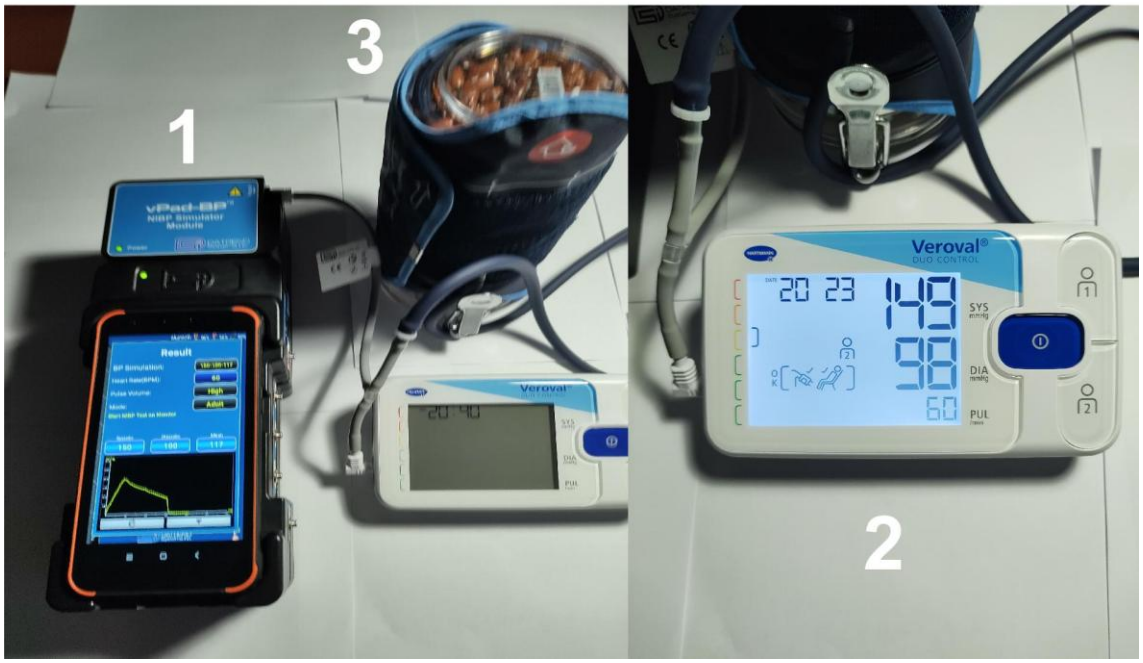

(**a**) (**b**)

Figure 10. Test setup used to calibrate the commercial home blood pressure monitor: (**a**) equipment interconnections (1—commercial and certified BP calibrator, 2—home blood pressure monitor, 3—dummy arm used to fix the ABPMD cuff); (**b**) front view of the home blood pressure monitor with an example of displayed measurement results.

The set of parametrizations used for the comparative performance evaluation between the BP calibrator prototype and the commercial and certified BP calibrator includes the following set of values for systolic and diastolic pressures and HBR: 30-15-22; 60-30-40; 80-50-60; 100-65-77; 120-80-93; 150-100-117; 200-150-167 and 255-195-205, respectively. Figures 11 and 12 represent the experimental results that were obtained for the six values of systolic BP.

From the calibration results, it is possible to see that regarding the calibration errors obtained by the commercial and certified BP calibrator, the maximum absolute error is lower than 2 mmHg, which corresponds to a maximum relative error almost equal to 1.4% relative to the pressure measurement range that is equal to 140 mmHg. Regarding the calibration errors obtained with the calibrator prototype, the maximum absolute error is a little bit higher but still lower than 3.6 mmHg, which corresponds to a maximum relative error almost equal to 2.6% relative to the same pressure measurement range. Moreover, it is also important to underline that the Pearson correlation coefficient values that were obtained with the commercial and certified BP calibrator and with the calibrator prototype were equal to 0.999 and 0.997, respectively. In both cases, the calibration results that were obtained verify the pass clinical validation criteria that, according to the British Hypertension Society (BHS), require mean and standard deviation errors, against the gold standard, to be lower than ±5 mmHg and 8 mmHg, respectively.

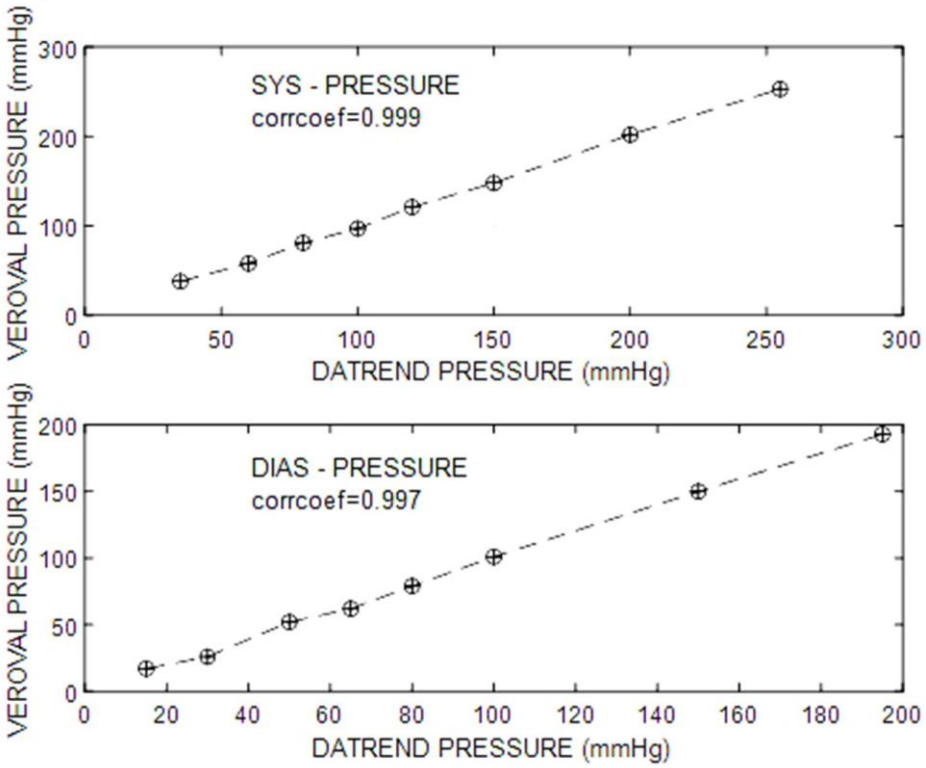

Figure 11. Calibration results of the home BP monitor (VEROVAL) when the calibration is performed with a commercial and certified BP calibrator (DATATREND).

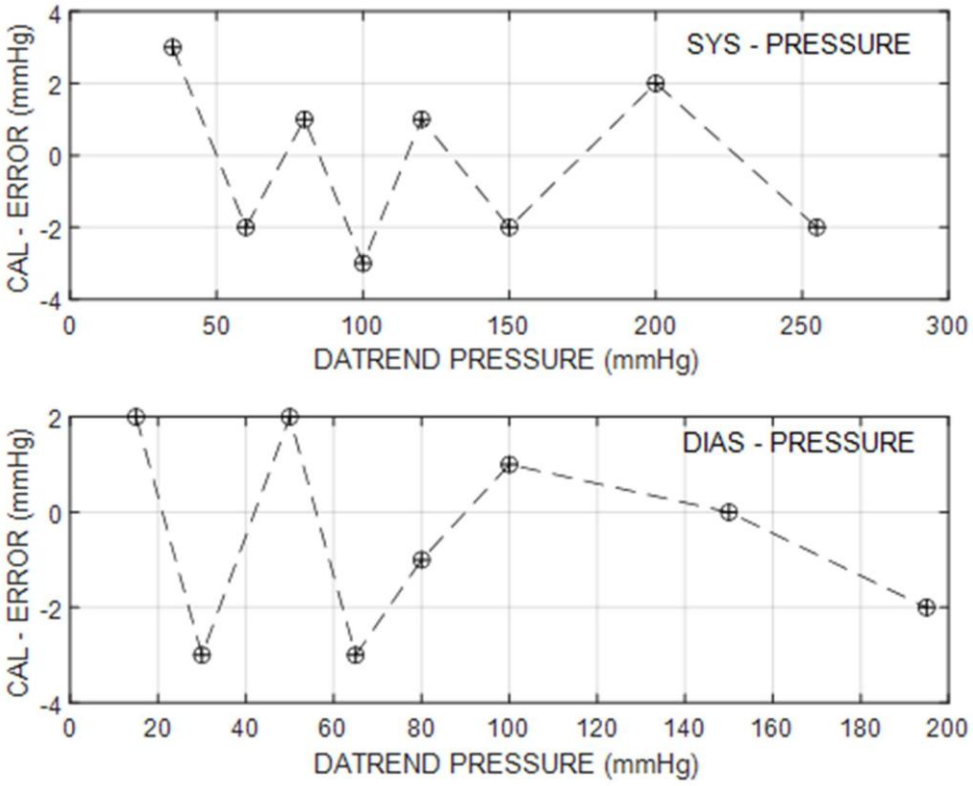

Figure 12. Calibration results of the home BP monitor (VEROVAL) when the calibration is performed with the proposed BP calibrator prototype.

5. Conclusions

This paper presents an NIBP calibrator that aims to assess oscillometric testing results without being affected by the empirical proprietary algorithms used by the different ABPMD manufacturers. By adjusting the pulse envelope signal used for the evaluation of the systolic and diastolic pressures, users can simulate different blood pressure parameters and test how different NIBP monitors respond to those signals. Another interesting characteristic of the proposed NIBP calibrator is related to the feedback topology of the proposed prototype that enables easy implementation of auto-calibration and auto-testing capabilities, which are essential in assuring accurate measurements as well as detecting faulty equipment conditions of a BP calibrator. This feedback topology enables dual capabilities of pressure stimulation and pressure measurement, with it also being possible to mimic the pressure patterns or pressure signatures previously acquired and to perform not only the ABPMD test but also the complete test of the pressure measuring channel, which includes the pneumatic channel, devices connecting the tubing and pneumatic loads, as is the case of the BP measuring cuff. This capability is important not only for other biomedical applications, such as the non-nutritive sucking measurement and stimulation of premature babies, but also for other applications where the accuracy of the measurement of time-variable pressure signals is essential. Simulation and experimental results that were obtained validate the theoretical expectations and show a very acceptable level of accuracy and performance of the presented NIBP calibrator prototype. Future work must be targeted at validating the proposed prototype using a larger number of BP monitors and calibrators from different certified manufacturers and at validating their algorithms using patient data, real human data and available blood pressure datasets to obtain a more complete characterization of the proposed prototype, identify potential limitations and study the best way to surpass them.

Author Contributions: Conceptualization, J.M.C.D.P., O.P. and G.R.; methodology, J.M.C.D.P.; software, J.M.C.D.P.; validation, J.M.C.D.P. and O.P.; formal analysis, J.M.C.D.P. and O.P.; investigation, J.M.C.D.P. and O.P.; resources, J.M.C.D.P., O.P. and G.R.; data curation, J.M.C.D.P., O.P. and G.R.; writing— J.M.C.D.P., O.P. and G.R.; writing—review and editing, J.M.C.D.P.; visualization, J.M.C.D.P., O.P. and G.R.; supervision J.M.C.D.P.; project administration, J.M.C.D.P. and O.P.; funding acquisition, J.M.C.D.P. and O.P. All authors have read and agreed to the published version of the manuscript.

Funding: This work is funded by FCT/MECI through national funds and co-funded EU funds under UID/50008: Instituto de Telecomunicações.

Institutional Review Board Statement: Not applicable.

Data Availability Statement: The original contributions presented in this study are included in the article. Further inquiries can be directed to the corresponding author.

Conflicts of Interest: The authors declare no conflicts of interest.

References

1. Timmis, A.; Townsend, N.; Gale, C.P.; Torbica, A.; Lettino, M.; Petersen, S.E.; Mossialos, E.A.; Maggioni, A.P.; Kazakiewicz, D.; May, H.T.; et al. Cardiovascular Disease Statistics 2019. European Society of Cardiology. *Eur. Heart J.* **2020**, *41*, 12–85. [CrossRef] [PubMed]
2. Unger, T.; Borghi, C.; Charchar, F.; Khan, N.A.; Poulter, N.R.; Prabhakaran, D.; Ramirez, A.; Schlaich, M.; Stergiou, G.S.; Tomaszewski, M.; et al. International Society of Hypertension Global Hypertension Practice Guidelines. *Hypertension* **2020**, *75*, 6. [CrossRef]
3. John, O.; Campbell, N.R.; Brady, T.M.; Farrell, M.; Varghese, C.; Berumen, A.V.; Gaitan, L.A.V.R.; Toffelmire, N.; Ameel, M.; Mideksa, M.; et al. The 2020 "WHO Technical Specifications for Automated Non-Invasive Blood Pressure Measuring Devices With Cuff". *Hypertension* **2021**, *77*, 806–812. [CrossRef]

4. Ma, Y.; Chen, Y.; Ma, Y.; Feng, X. The effect of arterial stiffness on cuff-based blood pressure measurement. *Extrem. Mech. Lett.* **2021**, *48*, 101298. [CrossRef]
5. Muntner, P.; Shimbo, D.; Carey, R.M.; Charleston, J.B.; Gaillard, T.; Misra, S.; Myers, M.G.; Ogedegbe, G.; Schwartz, J.E.; Townsend, R.R.; et al. Measurement of Blood Pressure in Humans: A Scientific Statement From the American Heart Association. *Hypertension* **2019**, *73*, e35–e66. [CrossRef]
6. Stergiou, G.S.; Dolan, E.; Kollias, A.; Poulter, N.R.; Shennan, A.; Staessen, J.A.; Zhang, Z.; Weber, M.A. Blood pressure measurement in special populations and circumstances. *J. Clin. Hypertens.* **2018**, *20*, 1122–1127. [CrossRef] [PubMed]
7. Picone, D.S.; Deshpande, R.A.; Schultz, M.G.; Fonseca, R.; Campbell, N.R.C.; Delles, C.; Olsen, M.H.; Schutte, A.E.; Stergiou, G.; Padwal, R.; et al. Nonvalidated Home Blood Pressure Devices Dominate the Online Marketplace in Australia: Major Implications for Cardiovascular Risk Management: Hypertension. *Hypertension* **2020**, *75*, 1593–1599. [CrossRef] [PubMed]
8. Sharman, J.E.; Tan, I.; Stergiou, G.S.; Lombardi, C.; Saladini, F.; Butlin, M.; Padwal, R.; Asayama, K.; Avolio, A.; Brady, T.M.; et al. Automated oscillometric blood pressure measuring devices: How they work and what they measure. *J. Hum. Hypertens.* **2023**, *37*, 93–100. [CrossRef] [PubMed]
9. Kumar, S.; Yadav, S.; Kumar, A. Oscillometric Waveform Evaluation for Blood Pressure Devices. *Biomed. Eng. Adv.* **2022**, *4*, 100046. [CrossRef]
10. Celler, B.G.; Argha, A.; Le, P.N.; Ambikairajah, E. Novel methods of testing and calibration of oscillometric blood pressure monitors. *PloS ONE* **2018**, *13*, e0201123. [CrossRef]
11. Rigel Medical GMC Instruments Group. What Are 'O Curves' and How Do I Create Them? Available online: https://www.rigelmedical.com/gb/support/patient-simulation (accessed on 31 December 2024).
12. Fluke. ProSim 8 Vital Signs Patient Simulator. 2011. Available online: https://www.flukebiomedical.com (accessed on 31 December 2024).
13. National Standards Authority of Ireland (NSAI). Developing an Infrastructure for Improved and Harmonised Metrological Checks of Blood-Pressure Measurements in Europe. National Metrology Laboratory (NML), Dublin. Available online: https://shop.standards.ie/en-ie/search/standard/?searchTerm=adOSSIG (accessed on 17 February 2025).
14. Geršak, G.; Schiebl, M.; Nawotka, M.; Jugo, E.; Ferreira, M.D.C.; Duffy, A.; Rosu, D.M.; Pavlásek, P.; Sedlák, V.; Pražák, D. Physiology-based patient simulator for blood pressure meter testing. *Meas. Sens.* **2021**, *18*, 100260. [CrossRef]
15. Sedlák, V.; Pražák, D.; Tesař, J.; Rosu, D.; Geršak, G.; Ferreira, M.; Nawotka, M.; Bosnjakovic, A.; Jugo, E.; Hetherington, P.; et al. Evaluation of Sphygmomanometers Using an Advanced Oscillometric Signal Generator. In Proceedings of the Imeko TC11 & TC24 Joint Hybrid Conference, Dubrovnik, Croatia, 17–19 October 2022; pp. 12–16.
16. Balestrieri, E.; Rapuano, S. Instruments and Methods for Calibration of Oscillometric Blood Pressure Measurement Devices. *IEEE Trans. Instrum. Meas.* **2010**, *59*, 2391–2404. [CrossRef]
17. Ratnadewi; Ramdhani, M.F.; Kurniasih, N.; Putri, L.D.; Parwito; Abdullah, D.; Listyorini, T.; Bakhtiar, M.I.; Nanuru, R.F.; Rahim, R. Automatic Blood Pressure Detector Using Arduino to Measure Blood Pressure in Indonesian People Age 19–27 Years Old. *Int. J. Eng. Technol.* **2018**, *7*, 115–118.
18. Chandrasekhar, A.; Yavarimanesh, M.; Hahn, J.-O.; Sung, S.-H.; Chen, C.-H.; Cheng, H.-M.; Mukkamala, R. Formulas to Explain Popular Oscillometric Blood Pressure Estimation Algorithms. *Front. Physiol.* **2019**, *10*, 1415. [CrossRef]
19. Dhamotharan, V.; Chandrasekhar, A.; Cheng, H.-M.; Chen, C.-H.; Sung, S.-H.; Landry, C.; Hahn, J.-O.; Mahajan, A.; Shroff, S.G.; Mukkamala, R. Mathematical Modeling of Oscillometric Blood Pressure Measurement: A Complete, Reduced Oscillogram Model. *IEEE Trans. Biomed. Eng.* **2023**, *70*, 715–722. [CrossRef] [PubMed]
20. Mauck, G.W.; Smith, C.R.; Geddes, L.A.; Bourland, J.D. The Meaning of the point of maximum oscillations in cuff pressure in the indirect measurement of blood-pressure—Part II. *Trans. ASME* **1980**, *102*, 28–33. [CrossRef]
21. Drzewiecki, G.; Hood, R.; Apple, H. Theory of the oscillometric maximum and the systolic and diastolic detection ratios. *Ann. Biomed. Eng.* **1994**, *22*, 88–96. [CrossRef] [PubMed]
22. Geddes, L.A.; Voelz, M.; Combs, C.; Reiner, C.; Babbs, C.F. Characterization of the oscillometric method for measuring indirect blood pressure. *Ann. Biomed. Eng.* **1982**, *10*, 271–280. [CrossRef]
23. Bronzino, J.D. *Medical Devices and Systems*; Taylor & Francis: Abingdon, UK, 2006.
24. Forouzanfar, M.; Dajani, H.R.; Groza, V.Z.; Bolic, M.; Rajan, S.; Batkin, I. Oscillometric blood pressure estimation: Past, present, and future. *IEEE Rev. Biomed. Eng.* **2015**, *8*, 44–63. [CrossRef]
25. National High Blood Pressure Education Program/National Heart. The Seventh Report of the Joint National Committee on Prevention, Detection, Evaluation, and Treatment of High Blood Pressure. *Hypertension* **2003**, *289*, 2560–2571.
26. Alpert, M.D.; Quinn, D.; Gallick, D. Oscillometric blood pressure: A review for clinicians. *J. Am. Soc. Hypertens.* **2014**, *8*, 930–938. [CrossRef] [PubMed]
27. Fei, D.; Deng, C. Novel Method for More Precise Determination of Oscillometric Pulse Amplitude Envelopes. *Comput. Inf. Sci.* **2015**, *8*, 64. [CrossRef]

28. Mafi, M.; Rajan, S.; Bolic, M.; Groza, V.Z.; Dajani, H.R. Blood pressure estimation using maximum slope of oscillometric pulses. In Proceedings of the 2012 Annual International Conference of the IEEE Engineering in Medicine and Biology Society, San Diego, CA, USA, 28 August–1 September 2012.
29. Barrios-Fernandez, S.; Sosa-Sánchez, E.M.; Muñoz-Bermejo, L.; Morenas-Martín, J.; Apolo-Arenas, M.D.; Adsuar, J.C.; Domínguez-Muñoz, F.J. Intrasession Reliability Analysis for Oscillometric Blood Pressure Method Using a Digital Blood Pressure Monitor in Peruvian Population. *Healthcare* **2022**, *10*, 209. [CrossRef] [PubMed]
30. Fonseca-Reyes, S.; Romero-Velarde, E.; Torres-Gudiño, E.; Illescas-Zarate, D.; Forsyth-MacQuarrie, A.M. Comparison of auscultatory and oscillometric BP measurements in children with obesity and their effect on the diagnosis of arterial hypertension. *Arch. Cardiol. Mex.* **2018**, *88*, 16–24. [CrossRef]
31. NXP Semiconductors. Document Number: MP3V5050. Data Sheet: Technical Data Rev. 1.4. 2018. Available online: https://www.nxp.com/docs/en/data-sheet/MP3V5050.pdf (accessed on 31 December 2024).
32. Parker. *Miniature Electronic Pressure Regulators—Precision Fluidcs*; Parker: Mayfield Heights, OH, USA, 2018.
33. Koge Micro Tech Co., Ltd. Selenoid Valve, KSV05 Series. Available online: https://www.koge.com/ (accessed on 31 December 2024).
34. ARDUINO. Arduino UNO WIFI REV2. Available online: https://store.arduino.cc/en-pt/products (accessed on 31 December 2024).
35. Air Flow Developments Ltd. FL 1.5 Manometer. Available online: https://www.bsria.com/doc/Bv6AdB/ (accessed on 31 December 2024).
36. Keithley. Keithley 2000 Series: 6½-Digit Multimeter with Scanning. Available online: https://www.tek.com/tektronix-and-keithley-digital-multimeter (accessed on 31 December 2024).
37. National Instruments. MyDAQ Data Acquisition Board. Available online: https://www.ni.com/pt (accessed on 31 December 2024).
38. General Electric Company. Measurement and Control. Druck DPI611—Portable Pressure Calibrator. Available online: https://www.neoinstruments.com (accessed on 31 December 2024).
39. Li, Y.; Li, F.; Li, Y.; Cui, X.; Li, J.; Zhi, H.; Wang, W.; Sun, Y.; Cui, W. Effect of cuff positioning on the accuracy of blood pressure measurement with automated electronic blood pressure monitors. *J. Clin. Hypertens.* **2020**, *22*, 1163–1172. [CrossRef]
40. Savitzky, A.; Golay, M.J.E. Smoothing and differentiation of data by simplified least squares procedures. *Anal. Chem.* **1964**, *36*, 1627–1639. [CrossRef]
41. Paul Hartmann, A.G. Veroval DUO CONTROL. Available online: https://www.veroval.info/en-ae/technology (accessed on 31 December 2024).
42. DATREND Systems. Vpad-BP NIBP Simulator. Available online: https://www.datrend.com/product/vpad-bp/ (accessed on 31 December 2024).
43. O'Brien, E.; Petrie, J.; Littler, W.; de Swiet, M.; Padfield, P.L.; O'Malley, K.; Jamieson, M.; Altman, D.; Bland, M.; Atkins, N. Protocol for the evaluation of automated and semi-automated blood pressure measuring devices with special reference to ambulatory systems. *J. Hypertens.* **1990**, *8*, 607–619. [CrossRef]
44. GE Healthcare—Product Specifications—DINAMAP® PRO 300. Vital Signs Monitor, DINAMAP® PRO 300 Vital Signs Monitor. Available online: https://www.medlikim.com/wp-content/ (accessed on 31 December 2024).

Disclaimer/Publisher's Note: The statements, opinions and data contained in all publications are solely those of the individual author(s) and contributor(s) and not of MDPI and/or the editor(s). MDPI and/or the editor(s) disclaim responsibility for any injury to people or property resulting from any ideas, methods, instructions or products referred to in the content.